

**High-energy optical response of artificial opals**

J. F. Galisteo-López and C. López\*

*Instituto de Ciencia de Materiales de Madrid, Cantoblanco 28049-Madrid, Spain*

(Received 24 February 2004; published 20 July 2004)

A detailed experimental study of the optical properties in the high-energy region (up to  $a/\lambda=1.8$ ) of high-quality artificial opals is performed by means of reflection and transmission spectroscopy. A number of issues, such as scalability and finite size effects, are taken into account before tentative comparison with theory is carried out. The experimental system under study is further modified by a controlled filling of the interstitials between the spheres, and its optical properties monitored throughout the process. We observe that the main features of the optical response of artificial opals seem to be accounted for by bands originated by wave vectors parallel to the  $\Gamma L$  direction and their perturbations, such as gaps opening at the center and edges of the Brillouin zone and anticrossings elsewhere, introduced through the interaction with other bands of similar energy and symmetry. This work constitutes an experimental approach to understand the interaction of light with photonic bands which introduces a challenge for future experimental and theoretical work.

DOI: 10.1103/PhysRevB.70.035108

PACS number(s): 42.70.Qs, 42.25.Fx, 42.25.Gy

**I. INTRODUCTION**

Photonic crystals<sup>1,2</sup> (PC's) are artificial dielectric materials with a spatially periodic refractive index. If electromagnetic radiation with a wavelength of the order of the period propagates inside a PC, it will be multiply scattered. For a given direction, constructive interference of the scattered light may forbid the propagation within a certain frequency range, commonly known as a stop band. The extent of this range depends on the scattering strength of the periodic lattice, which can be controlled through the refractive index contrast as well as through the topology of the structure. For a sufficiently large contrast and appropriate crystal symmetry, stop bands can be made broad enough to overlap every direction of propagation. This would lead to the formation of a photonic band gap (PBG): a range of frequencies where no electromagnetic modes exist for the PC.

Among the many approaches developed to fabricate 3D PC's,<sup>3</sup> artificial opals<sup>4,5</sup> are probably the most popular ones. This is due to the ease and low cost of the process, based on the natural tendency of monodisperse glass or polymer beads to self assemble into fcc arrays. Although the underlying structure present in these systems prevents them from having a PBG regardless of refractive index of the spheres, a complete PBG may be achieved by infiltrating the opal with a high refractive index material and subsequently removing the original matrix.<sup>6</sup> Moreover, artificial opals have been demonstrated to be an ideal starting point for fabricating more complex structures such as photonic fibers<sup>7</sup> and planar optical cavities.<sup>8</sup>

Whether grown by natural sedimentation<sup>5</sup> or vertical deposition,<sup>9</sup> artificial opals present their surface parallel to the  $\{111\}$  family of crystallographic planes. Thus, it is the  $\Gamma L$  direction in reciprocal space that is usually probed in optical characterization experiments such as transmission and reflection measurements at normal incidence. While these systems have been extensively studied as photonic crystals for nearly a decade now, most experimental studies have concentrated on the behavior of the low-energy region of the band structure ( $a/\lambda\sim 0.5$ ) (where  $a$  is the lattice pa-

rameter and  $\lambda$  the wavelength of light). In this region, the crystal presents a stop band as a consequence of Bragg diffraction by the  $\{111\}$  planes, and may be treated as an effective medium for frequencies surrounding the stop band.<sup>10</sup> For energies above this stop band, although some experimental results have been presented for opal based PC's,<sup>6,11-16</sup> most of them were concerned with identifying the reflectivity peak through which the PBG should manifest<sup>6,12-14</sup> in inverse opals with a sufficiently high refractive index contrast. For titania inverse opals a number of features were observed in reflectivity spectra and successfully accounted for by theoretical band calculations,<sup>11</sup> identifying the precursor for a PBG. But the interest in this energy region does not just lie on the existence of stop bands. Spectacular phenomena such as the superprism effect<sup>17</sup> may be observed in artificial opals<sup>18</sup> for frequencies where many energy bands overlap, and their behavior is radically different from the linear one observed in the surroundings of the (111) pseudogap. From a more fundamental point of view, the understanding of the complex interaction between electromagnetic radiation and energy bands in this region lies at the very heart of a solid-state physics approach to PC.

In this work we report a detailed study of the optical response of artificial opals for energies between  $a/\lambda=0.9$  and  $a/\lambda=1.8$ . In this region one would expect the second and third order Bragg diffractions associated with the  $\{111\}$  planes, if these planes were the only to interact with the incident light. As will be seen, the situation is more complex. The optical characterization is carried out by means of normal incidence reflection and transmission measurements. In order to ensure that the experimental features we observe come solely from the interaction of electromagnetic radiation with the energy bands of the crystal, a number of issues are taken into account such as dispersion in the refractive index of the spheres, scalability of the features and finite size effects. A qualitative comparison is then carried out with calculated energy bands.<sup>19</sup> By filling the interstitials between the spheres with  $\text{SiO}_2$  in a controlled manner, the optical properties of the system are modified and its evolution monitored and compared with theory. We propose that the optical

response of our system for light impinging in the (111) direction can be accounted for mainly by the photonic bands originating from the dispersion relation with  $\mathbf{k}$  vectors parallel to the  $\Gamma L$  direction ( $\Gamma L$  bands hereafter) and its perturbations. These perturbations are splittings (at the center and edges of the Brillouin zone) and anticrossings caused by interaction with bands associated with  $\mathbf{k}$  vectors originally not parallel to the  $\Gamma L$  direction but made so upon folding back into the Brillouin zone by reciprocal lattice vectors. The description is completed by the coupling of light with the latter bands, dispersionless in certain frequency ranges. A very similar behavior has been theoretically described for two-dimensional (2D) photonic crystals.<sup>20</sup> Experimental results for artificial opals on the high-energy region have appeared as angle resolved transmission in a reduced interval ( $1 \leq a/\lambda \leq 1.3$ ),<sup>16</sup> and normal incidence transmission<sup>13,15,16</sup> for the wider range considered here but, to the best of our knowledge, no in depth study has been carried out in order to interpret the optics in this energy range.

## II. EXPERIMENTAL

Thin film artificial opals were fabricated by the vertical deposition method<sup>9</sup> starting from aqueous solutions of polystyrene spheres of several diameters. Further information on the fabrication procedure can be found elsewhere.<sup>21</sup> Normal incidence reflection and transmission measurements were carried out with a microscope attached to a FTIR spectrometer (BRUKER IFS 66/S). In both types of measurements, a spot with a diameter  $375 \mu\text{m}$  was probed. InSb and silicon detectors were employed to detect light in the near infrared and visible part of the spectrum.  $\text{SiO}_2$  infilling of the opal interstitials was carried out in a controlled manner with a CVD line working at room temperature and atmospheric pressure.<sup>22</sup> The refractive index of the grown  $\text{SiO}_2$ , as estimated by ellipsometry, was found to be similar to that of fused  $\text{SiO}_2$ .<sup>23</sup>

## III. SCALABILITY OF SPECTRAL FEATURES

The main problems encountered when probing the optical properties of artificial opals in the high-energy range above the (111) stop band, are related to disorder and multiple Bragg diffraction. In this energy range, the wavelength of the probing light is smaller than the sphere diameter and therefore likely to be scattered by imperfections in the unit cell which would hardly affect the measurements in the lower-energy region. Thus, high-quality samples are needed in order to minimize these effects. Also, the band structure for such high frequencies becomes complicated. In the low-energy region, for  $a/\lambda < 1$ , the band structure consists of two sets of degenerate bands having a constant slope and being a reminiscence of the effective medium dispersion relation. At the edge of the Brillouin zone a breaking up of the vacuum-like dispersion relation occurs leading to the opening of the  $L$  gap due to Bragg diffraction by the  $\{111\}$  family of planes. But for higher frequencies the situation becomes more complex. The appearance of bands arising from wave-vectors originally not parallel to the  $\Gamma L$  direction but folded back

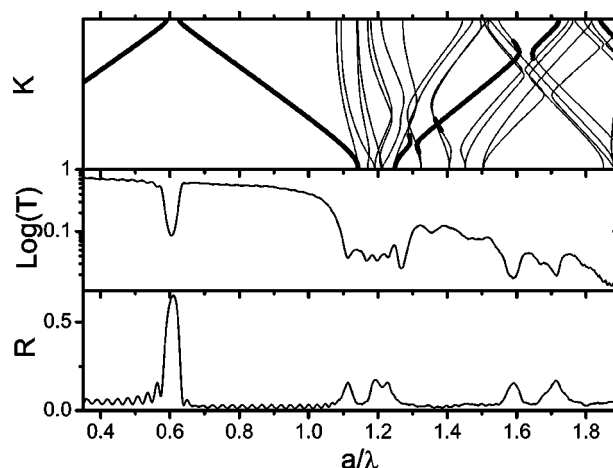


FIG. 1. Band structure calculated along the  $\Gamma L$  direction in reciprocal space for an artificial opal consisting of polystyrene spheres (top).  $\Gamma L$  bands are highlighted with thick lines. Transmission (middle) and reflection (bottom) spectra at normal incidence for an artificial opal 21 layers thick.

into the first Brillouin zone by translational symmetry introduces anticrossings between bands of same energy and symmetry.<sup>20</sup> Also, higher order Bragg diffractions by the  $\{111\}$  planes are expected. This complicates the band structure making the comparison between experimental spectra and calculated bands a nontrivial task. The above can be appreciated in Fig. 1, where transmission and reflection spectra at normal incidence for a polystyrene artificial opal 21 layers thick are plotted together with the calculated band structure. In the latter, the  $\Gamma L$  bands have been highlighted. For reduced frequencies  $a/\lambda < 1$ , the experimental spectra present a well known behavior consisting of a reflectance peak accompanied by a dip in transmission, corresponding to those frequencies contained in the stop band. Out of these frequencies, where the dispersion relation can be approximated to a linear regime, transparency windows in reflection and transmission are found. Although for the latter a monotonic decrease in intensity can be appreciated, the origin of which is to be found in Rayleigh scattering and several sources of disorder present in the crystal.<sup>24</sup> In the high-energy region, for  $a/\lambda > 1$ , a different behavior can be appreciated with a strong decrease in transmission and a number of features both, in transmission and reflection. This regime coincides with a dramatic change in the band structure of the system, which presents a complicated intermixture of energy bands.

The origin of the above mentioned features in the photonic band structure was confirmed by comparing experimental spectra for samples having different diameters (between 500 and 700 nm) with the same number of layers and confirming the scalability of the features. Figure 2 shows reflectivity spectra in the high-energy region for samples having 505 and 695 nm diameter spheres. It can be seen that both spectra present identical features, although a small redshift is present in the spectrum corresponding to the smaller spheres, which increases towards higher energies. This shift can be explained in terms of the polystyrene refractive index dispersion. Bulk polystyrene presents a normal dispersion,<sup>25</sup> so it

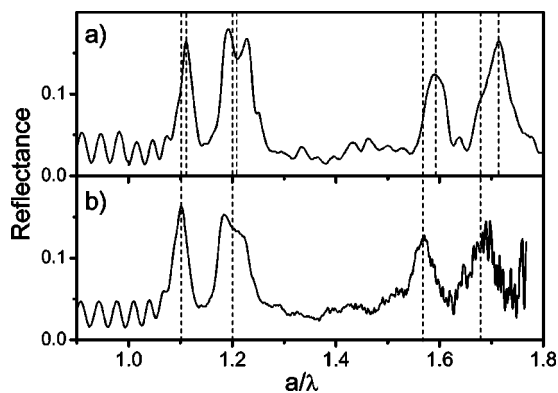


FIG. 2. Reflectivity spectra in the high energy region for two samples consisting of 695 (a) and 505 nm (b) diameter spheres. Dashed vertical lines indicate the position of the main optical features for each spectrum.

can be expected that, as we move towards higher energies, its refractive index will increase more dramatically. It is reasonable then that as the diameter of the spheres decreases, the high-energy features will move towards the highly dispersive spectral region, thus presenting an increasing redshift with respect to the ones obtained from larger spheres. Therefore, if we take into account this dispersion in the dielectric constant, together with the fact that polystyrene does not absorb for these frequencies<sup>26</sup> we may conclude that the observed features are caused by interaction of incident light with photonic bands. In order to compare experimental spectra with calculated bands we will use the larger spheres, as the variation in refractive index is smaller. If we assume the refractive index of our spheres to be that of bulk polystyrene, in the spectral region where the high-energy features are found (between 0.55 and 0.98  $\mu\text{m}$ ) it will vary between 1.592 and 1.573. Since the numeric algorithm employed to calculate energy bands<sup>19</sup> does not allow the introduction of dispersion in the refractive index of the constituent materials, we have chosen a mean value of 1.58.

#### IV. FINITE SIZE EFFECTS

We have performed a study of the behavior of the optical response of our samples as a function of the number of layers in order to avoid spurious effects associated to the finite size of the samples in subsequent analysis. Figure 3 shows reflectivity spectra for samples fabricated with the 695 nm diameter spheres, for increasing number of layers. For samples 4 layers thick the reflectivity spectra presents a fringelike pattern similar to that of transparent homogeneous thin films. As the thickness increases to seven layers and beyond, some optical features are reinforced at the expense of others (Fabry Perot fringes) and remain for thicker samples: two reflectivity peaks centered around  $a/\lambda=1.1$  and 1.2, the latter presenting two shoulders, a low reflectance region between  $a/\lambda=1.27$  and 1.53, and two more peaks centered around  $a/\lambda=1.6$  and 1.72. For samples 14 layers thick, the above mentioned peaks have reached a stationary line shape and spectral position, as well as a reflectance (of about 15%), which will not change for samples as thick as 40 layers (not

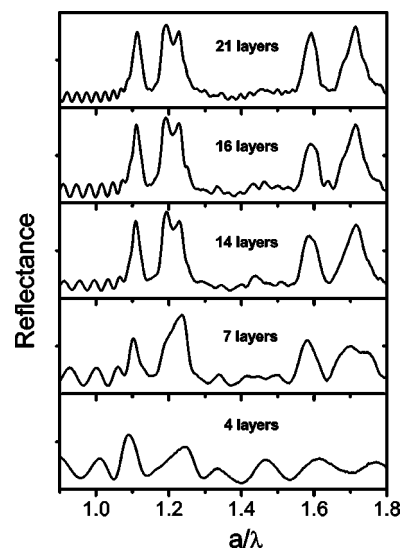


FIG. 3. Reflectance spectra for samples with an increasing number of layers. Bottom to top: 4, 7, 14, 16, and 21 layers. Reflectance goes from 0 to 0.2 in all graphs.

shown). It is worth noticing that, for an identical system, but in the low-energy region, structures consisting of 35 layers were needed to reach this infinite-crystal stationary behavior, avoiding finite size effects.<sup>21</sup>

#### V. COMPARISON WITH THEORY: BARE OPALS

In order to gain further understanding on the described behavior, reflectance and transmittance spectra are compared with calculated energy bands. The band structure was calculated for a refractive index of 1.58, the mean value in the variation range for these frequencies. This is shown in Fig. 4 for a sample 21 layers thick. We see how the reflectivity peaks at  $a/\lambda=1.1$  and 1.2, peaks 1 and 2 hereafter, are accompanied by a region of low transmission. Peak 1 appears in a region where the low-energy  $\Gamma L$  bands coexist with bands presenting a very small slope. The nature of this peak

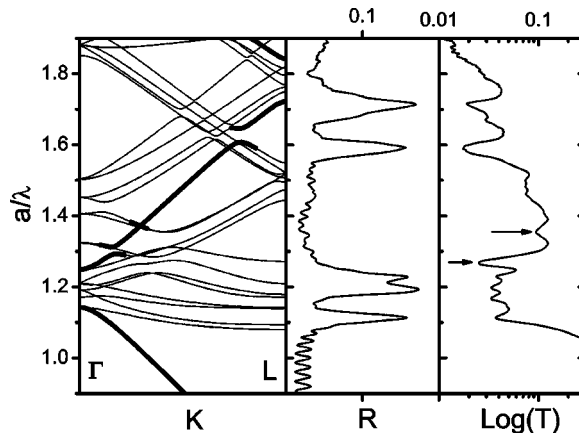


FIG. 4. High-energy bands calculated for a refractive index of 1.58 (left). Reflection (middle) and transmission (right) spectra for a 21 layers thick sample.

is clearly different from that of the Bragg peak ( $a/\lambda=0.6$ ) since in the latter, no states were available at the corresponding frequency. The effect of uncoupled modes, which cannot be excited by external light for symmetry reasons, can also be ruled out since, for these frequencies, uncoupled modes always coexist with allowed ones.<sup>27</sup> A plausible explanation for this behavior could be the coupling of light to energy bands presenting a low dispersion,<sup>16</sup> i.e., flat bands which are present in this part of the band structure. It has been predicted<sup>20</sup> that in the frequency region where such flat bands are found, the PC behaves as an effective medium with a large refractive index, and correspondingly presents a high reflectivity. Peak 2 corresponds to the region of the band structure where the  $\Gamma L$  bands split at the center of the Brillouin zone at frequencies where the second order Bragg diffraction would be expected to take place. Contrary to the splitting caused by the first order Bragg diffraction, here the gap is filled with photonic states. As for peak 1, these states correspond to flat bands, and therefore the origin of the reflection/transmission could be due to an effective medium behavior with a large refractive index.

In the frequency window between  $a/\lambda=1.27$  and  $1.53$ , the low reflectance is accompanied by a recovery of the transmission. If we observe this region as a function of the number of layers in Fig. 3, we can appreciate that reflectivity spectra appear as a set of fringes whose number increases with the thickness of the sample, indicating an effective refractive index medium behavior. This frequency interval corresponds to a region where the  $\Gamma L$  bands coexist with a number of bands having a different slope. At variance with what happens for frequencies above and below the pseudogap, where only two degenerate bands are found, unequivocally defining an effective refractive index, in this region a number of bands coexist for which reason defining a refractive index is not possible, as indicated by the fact that the fringes are not equidistant in frequency. In fact the incoming electromagnetic radiation is expected to couple, with different strengths, to all allowed modes for any given frequency.<sup>18</sup>

The two reflectivity peaks appearing at higher frequencies for  $a/\lambda=1.6$  and  $1.72$  (peaks 3 and 4 hereafter) find corresponding transmission dips in a spectral region where the  $\Gamma L$  bands undergo an anticrossing and a splitting at the edge of the Brillouin zone, respectively. The experimental features seem to be redshifted with respect to the calculated ones, which are centered at  $a/\lambda=1.627$  and  $1.783$ . This could be due to the fact that for such high frequencies the actual refractive index of polystyrene is larger than the value input to calculate the bands. The effect of band anticrossing on the optical properties of opal-based photonic crystals has been previously reported.<sup>21,28,29</sup> However, these studies were performed in a spectral region where few bands were present and the band repulsion involved the existence of stop bands. In the present case the situation is more complicated as the anticrossing region is filled with states distributed over several bands. A similar situation is found in the region with the splitting, which takes place for frequencies where the third order Bragg diffraction by the  $\{111\}$  planes would be expected. In both cases, assigning the optical features to either band is nontrivial. This and other issues, such as the presence of peak 1 in a spectral region where the effective medium

bands remain unperturbed could probably be understood if the exact coupling strength between the incident light and each band were calculated<sup>18</sup> which is desirable but out of the scope of the present work.

Finally we point out the existence of two transmission dips appearing at  $a/\lambda=1.27$  and  $1.35$ , less intense than the previous ones, and which cannot be appreciated in the reflection spectra. They are pointed out by arrows in Fig. 4. Again, these dips are found in a spectral region where two anticrossings take place at  $a/\lambda=1.3$  and  $1.37$  in the calculated bands. The attenuation of the former dip is larger than that of the latter, which agrees with the width of the corresponding anticrossings. These two dips will be referred to as peak 5 and 6 in subsequent analysis.

## VI. COMPARISON WITH THEORY: FILLED OPALS

A gradual transformation of the system towards a homogeneous material that allowed comparing it with a free photon model would lend itself useful in understanding the problem. In order to tune the optical response in a continuous fashion we had recourse to gradually infiltrating the structures with silica. This changes the average refractive index and, which is more important, it reduces the refractive contrast approaching the composite to a nearly homogeneous medium, providing a number of different topologies and band structures for comparison. Although silica presents a refractive index lower than that of polystyrene, so that the index matching condition is not met, the infiltration process<sup>22</sup> takes place at room temperature so that the polystyrene skeleton is not perturbed. Further, the silica growth takes place in a laminar way around the spheres, yielding samples whose band structure may be easily modeled provided the refractive index of both constituents is known. In this way we have made samples with pore fillings of 21, 34, 50, 66, and 80 % [close to the maximum filling of 86% (Ref. 22)]. The filling fraction was controlled through the comparison of the spectral position of the center of the Bragg peak with the center of the  $L$  gap in the calculated bandstructure, the former being the parameter less affected by finite size effects,<sup>21</sup> which are expected to become more pronounced as we decrease the refractive index contrast.

Figure 5 shows the evolution of the optical response of our system as we increase the pore filling fraction, reducing the contrast and increasing the average refractive index. All peaks shift to lower frequencies, owing to an increase in the average refractive index of the structure and, in general, present a decrease in intensity and spectral width due to the reduction of contrast. Peaks 1 and 3 show a most pronounced decrease in intensity as the contrast is reduced until they all but disappear for high fillings. On the other hand, peaks 2 and 4 remain more intense than the others, peak 2 losing its structure in the process. These features also have a correspondence in transmission experiments, as shown in Fig. 6 (two cases selected), and can be associated with the gaps opened in the  $\Gamma L$  bands at the center and boundaries of the Brillouin zone and elsewhere owing to anticrossings with other bands.

In transmission spectra we can also observe the two dips (peaks 5 and 6) associated with the anticrossings taking place

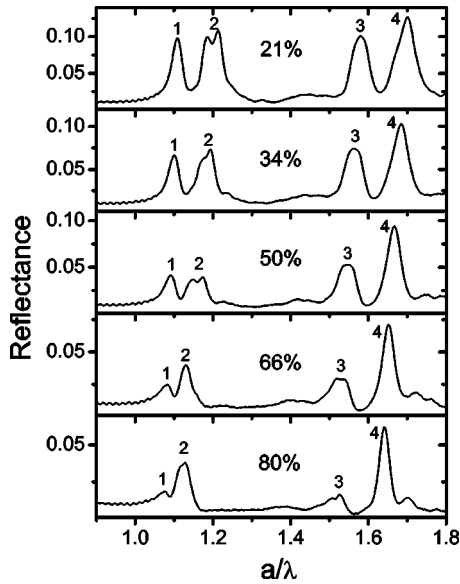


FIG. 5. Reflectivity spectra for a sample 35 layers thick with an increasing pore filling fraction. Peaks are labeled according to the text.

in the calculated bands near the center of the Brillouin zone for  $a/\lambda=1.27$  and  $1.35$  in the case of the bare opal. The strength of the interaction leading to the avoided crossing is determined by the scattering strength (refractive index contrast) narrowing and almost closing some of these gaps for high infiltration degrees. For a pore filling of 35% both of them are still present, but for 80% only the high-energy one is sizable enough to produce an attenuation band. The lower-energy one, narrower due to weakly interacting bands disappears as soon as the contrast is reduced. The anticrossing occurring close to the edge of the Brillouin zone at  $a/\lambda=1.6$  for bare opals (peak 3) survives even for the highest degrees of infiltration evincing strongly interacting bands.

Finally we compare the evolution of the experimental features with the calculated ones as the pore filling fraction is increased (Fig. 7). For the case of band splitting and anticrossings we have considered the center frequency as representative of the spectral position of the gap (anticrossing) at the edges and center of the Brillouin zone (elsewhere). For peak 1, associated with the flat bands,<sup>16</sup> we have chosen for comparison the frequency at which the bands become dispersionless close to the edge of the Brillouin zone. We can see how experimental results follow the same trend as calculated ones for an increasing pore filling fraction. The coincidence is satisfactory for all features although it can be appreciated that for those appearing at higher frequencies a marked redshift is still present in the experimental values. This was expected since for such high frequencies both materials constituting the crystal suffer an increase in refractive index.

VII. CONCLUSIONS

In conclusion, we have presented a detailed study of the optical behavior of artificial opals in the high-energy region above the pseudogap at the  $L$  point. After taking into account

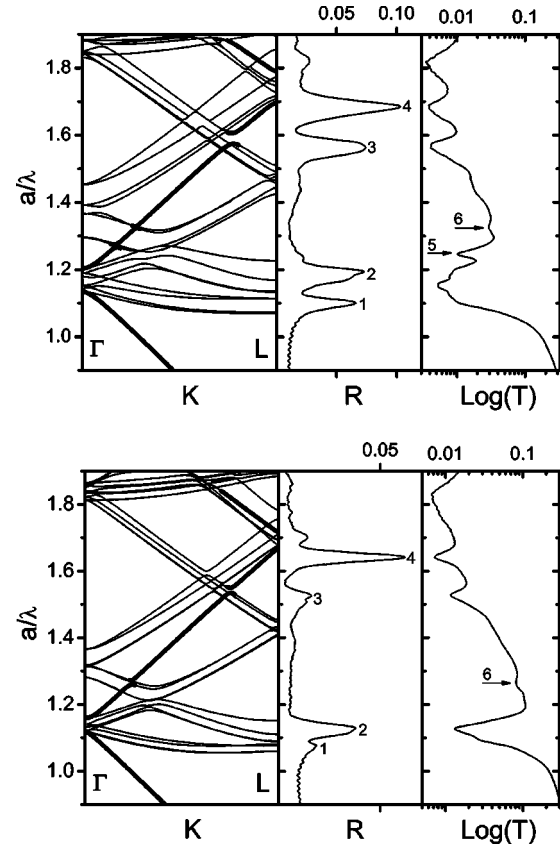


FIG. 6. Calculated band structure (left), and experimental reflectance (middle) and transmittance (right) for two samples having 35 (a) and 80% (b) of the pore filled with  $\text{SiO}_2$ . Peaks are labeled according to the text.

a number of issues such as scalability, refractive index dispersion and finite size effects, a tentative comparison was made with calculated energy bands. In order to continuously tune the photonic bands, the refractive index contrast of the samples was gradually lowered by filling the pores between

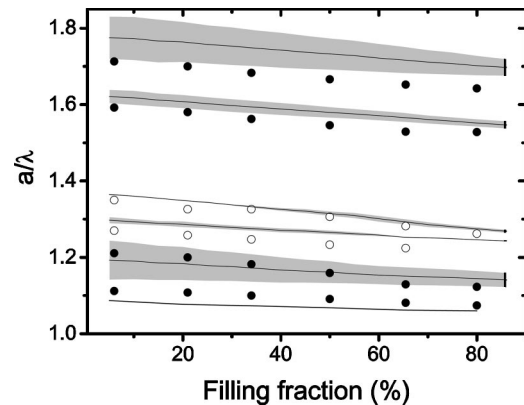


FIG. 7. Evolution of the spectral position of band anticrossing, splitting at the edges and center of the Brillouin zone and dispersionless bands. Open/closed symbols correspond to experimental data taken from transmission/reflection spectra. Lines/grey bands correspond to center/width of gaps and anticrossings extracted from theory.

the spheres. We propose that the optical response of artificial opals seems to be accounted for by the perturbations suffered by those bands originating from wave vectors parallel to the  $\Gamma L$  direction. These perturbations comprise both frequency splitting at the center and edges of the Brillouin zone, and anticrossings arising from interaction with bands of similar energy and symmetry coming from wavevectors originally not parallel to the  $\Gamma L$  direction but folded into the Brillouin zone by translational symmetry. In those regions where these bands are unperturbed, the crystal presents transparency windows, and a behavior similar to that of a homogeneous medium with Fabry-Perot fringes. On the other hand, for the frequency intervals where the abovementioned bands present anticrossings and splitting, the experimental spectra present reflection peaks accompanied by dips in transmission. The spectral position and peak width can be correlated to the average index and refractive contrast of the composite.

The present work constitutes a first approach to understand the complex interaction of electromagnetic radiation

with energy bands in the high energy region of PC, which recent techniques for band engineering<sup>30</sup> will certainly help to improve. It also highlights the need for a better understanding of the role played by flat bands as well as band anticrossings and splitting, which certainly introduces a challenge for future theoretical and experimental work.

#### ACKNOWLEDGMENTS

This work was partially financed by the Comunidad Autónoma de Madrid through Grant No. 07T/0048/2003 and Spanish MCyT through MAT 2003-01237 projects. We gratefully acknowledge E. Castillo-Martínez and E. Palacios-Lidón for bead synthesis, and L. Vázquez and R. Serna for technical help with silica dielectric characterization. The authors would like to thank Dr. F. García-Santamaría for fruitful discussions.

\*Electronic address: cefe@icmm.csic.es

- <sup>1</sup>E. Yablonovitch, Phys. Rev. Lett. **58**, 2085 (1987).
- <sup>2</sup>S. John, Phys. Rev. Lett. **58**, 2486 (1987).
- <sup>3</sup>C. López, Adv. Mater. (Weinheim, Ger.) **15**, 1679 (2003).
- <sup>4</sup>V. N. Astratov, V. N. Bogomolov, A. A. Kaplyanskii, A. V. Prokofiev, L. A. Samoilovich, S. M. Samoilovich, and Y. A. Vlasov, Nuovo Cimento D **17**, 1349 (1995).
- <sup>5</sup>R. Mayoral, J. Requena, S. J. Moya, C. López, A. Cintas, H. Míguez, F. Meseguer, L. Vázquez, M. Holgado, and A. Blanco, Adv. Mater. (Weinheim, Ger.) **13**, 409 (1997).
- <sup>6</sup>A. Blanco, E. Chomski, S. Grachtchak, M. Ibisate, S. John, S. W. Leonard, C. López, F. Meseguer, H. Míguez, J. P. Mondia, G. A. Ozin, O. Toader, and H. M. van Driel, Nature (London) **414**, 289 (2000).
- <sup>7</sup>H. Míguez, S. M. Yang, N. Tétreault, and G. A. Ozin, Adv. Mater. (Weinheim, Ger.) **14**, 1805 (2002).
- <sup>8</sup>E. Palacios-Lidón, J. F. Galisteo-López, B. H. Juárez, and C. López, Adv. Mater. (Weinheim, Ger.) **16**, 341 (2004).
- <sup>9</sup>P. Jiang, J. F. Bertone, K. S. Hwang, and V. L. Colvin, Chem. Mater. **11**, 2132 (1999).
- <sup>10</sup>K. W. Shung and Y. C. Tsai, Phys. Rev. B **48**, 11 265 (1993).
- <sup>11</sup>W. L. Vos and H. M. van Driel, Phys. Lett. A **272**, 101 (2000).
- <sup>12</sup>H. Míguez, E. Chomsky, F. García-Santamaría, M. Ibisate, S. John, C. López, F. Meseguer, J. P. Mondia, G. A. Ozin, O. Toader, and H. M. van Driel, Adv. Mater. (Weinheim, Ger.) **13**, 1634 (2001).
- <sup>13</sup>Y. A. Vlasov, X. Z. Bo, J. C. Sturm, and D. J. Norris, Nature (London) **414**, 289 (2001).
- <sup>14</sup>B. H. Juárez, M. Ibisate, J. M. Palacios, and C. López, Adv. Mater. (Weinheim, Ger.) **15**, 319 (2001).
- <sup>15</sup>K. Wostyn, Y. Zhao, B. Yee, K. Clays, and A. Persoons, J. Chem. Phys. **118**, 10 752 (2003).
- <sup>16</sup>H. Míguez, V. Kitaev, and G. A. Ozin, Appl. Phys. Lett. **84**, 1239 (2004).
- <sup>17</sup>H. Kosaka, T. Kawashima, A. Tomita, N. Notomi, T. Tamamura, T. Sato, and S. Kawakami, Phys. Rev. B **58**, R10 096 (1998).
- <sup>18</sup>T. Ochiai and J. Sánchez-Dehesa, Phys. Rev. B **64**, 245113 (2001).
- <sup>19</sup>Photonic band structures are computed using a plane wave basis in an iterative implementation as described in S. G. Johnson and J. D. Joannopoulos, Opt. Express **8**, 173 (2001). The calculations are performed for 60 bands and 100  $k$  points along the  $\Gamma L$  direction in reciprocal space.
- <sup>20</sup>K. Sakoda, *Optical Properties of Photonic Crystals* (Springer-Verlag, Berlin, 2001).
- <sup>21</sup>J. F. Galisteo-López, E. Palacios-Lidón, E. Castillo-Martínez, and C. López, Phys. Rev. B **68**, 115109 (2003).
- <sup>22</sup>H. Míguez, N. Tétreault, B. Hatton, S. M. Yang, D. Perovic, and G. A. Ozin, Chem. Commun. (Cambridge) **22**, 2736 (2002).
- <sup>23</sup>F. García-Santamaría, H. Míguez, M. Ibisate, F. Meseguer, and C. López, Langmuir **18**, 1942 (2002).
- <sup>24</sup>Yu. A. Vlasov, V. N. Astratov, O. Z. Karimov, A. A. Kaplyanskii, V. N. Bogomolov, and A. V. Prokofiev, Phys. Rev. B **55**, R13 357 (1997).
- <sup>25</sup>N. G. Sultanova, I. D. Nikolov, and C. D. Ivanov, Opt. Quantum Electron. **35**, 21 (2003).
- <sup>26</sup>T. Inagaki, E. T. Arakawa, R. N. Hamm, and M. W. Williams, Phys. Rev. B **15**, 3243 (1977).
- <sup>27</sup>F. López-Tejeira, T. Ochiai, K. Sakoda, and J. Sánchez-Dehesa, Phys. Rev. B **65**, 195110 (2002).
- <sup>28</sup>H. M. Van Driel and W. L. Vos, Phys. Rev. B **62**, 9872 (2000).
- <sup>29</sup>S. G. Romanov, T. Maka, C. M. Sotomayor Torres, M. Muller, R. Zentel, D. Cassagne, J. Manzanares-Martinez, and C. Jouanin, Phys. Rev. E **63**, 056603 (2002).
- <sup>30</sup>F. García-Santamaría, M. Ibisate, I. Rodríguez, F. Meseguer, and C. López, Adv. Mater. (Weinheim, Ger.) **15**, 788 (2003).